Current Topics in Peptide & Protein Research
Vol. 18, 2017

Original Communication

Nanoparticles and *Escherichia coli* prolyl-tRNA synthetase: Impact of Au and Ag nanoparticles on protein conformation and function

Stanford Mitchell*,#, Ashley Lato, Olivia Hurst, Lauren Adams, Jennifer Dahl and Sanchita Hati*,$
Department of Chemistry, University of Wisconsin – Eau Claire, Wisconsin, USA.

ABSTRACT

Nanoparticles have emerged as important tools in biomedicine, with numerous clinical applications including contrast agents in bioimaging and drug and gene delivery carriers. However, thorough investigation of their implications on biomolecular systems remain underexplored. Developing a functional knowledge of these interactions can be used to generate nanoparticles compatible with biological environments. The primary interest of this project has been to synthesize nanoparticles and study their impacts on the structure and function of an important family of enzymes known as aminoacyl-tRNA synthetases, which are responsible for attaching amino acids to a cognate tRNA molecule. Gold and silver nanoparticles, with ranging differences in core size and functionalization groups, were synthesized and purified using a variety of methods. Two unique biocompatible ligands were utilized, including citrate and 2-[2-(2-Mercaptoethoxy) ethoxy]ethanol. These nanoparticles were used to examine their impact on the conformation and function of *E. coli* prolyl-tRNA synthetase using intrinsic fluorescence spectroscopy and enzyme kinetics. The present study demonstrated that gold nanoparticles, regardless of diameter or functionalization, do not influence the conformation and function of *E. coli* prolyl-tRNA synthetase. On the other hand, silver nanoparticles have impact on the protein conformation but not the enzymatic function.

KEYWORDS: Au and Ag nanoparticles, prolyl-tRNA synthetase, intrinsic tryptophan fluorescence, enzyme kinetics, aminoacyl-tRNA synthetases, AARS activity.

1. INTRODUCTION

With nanotechnology emerging as a popular tool in biology and medicine, questions regarding its influence on the environment [1] and biological systems [2] remain underexplored. The physical and chemical properties of nanoparticles (NPs) are unique compared to those of bulk metal particles [3]; this has revolutionized the use of noble metals in biotechnology such as biosensing [4], drug delivery [5, 6], and biomedical imaging [7]. This has led to increased interest in NPs' impact on human health [8]. While NP toxicology is being explored [9], their impact on proteins and nucleic acids is of keen interest. Since NPs have excellent potential in medicine, understanding their impact on biomolecules is essential in the development of biologically safe and effective nanomedicine [10]. Further, knowledge of potential NP-induced conformational and functional changes in biomolecules may provide insight into NP toxicity mechanisms.

Proteins play critical roles in all aspects of life in the cell. NPs have been shown to alter protein folding [11] and functioning of enzymes [12].

*Corresponding authors
#sdmitchell3@wisc.edu
$hatis@uwec.edu

A corona, or film, of protein forms on the surface of NPs upon exposure to cells [13]. When enzymes become exposed to NPs and are incorporated onto a NP surface forming NP-protein corona, are their conformations and catalytic functions altered enough to impact the overall health of the cell, and further, the overall organism? This is a difficult question to answer given the complex nature of a living cell. Therefore, protein-NP interactions are exceedingly relevant in the discussion of physiological implications brought upon by NP exposure.

The aminoacyl-tRNA synthetases (AARSs) are an enzyme family responsible for attaching amino acids to their cognate tRNA molecules, an essential process for protein synthesis [14]. For each of the amino acids there exist a corresponding synthetase throughout all domains of life. Without even one synthetase, life would be significantly impaired since each amino acid is required to produce functional protein. If AARS functionality is impaired by the presence NPs, life of an organism may suffer. With the field of nanotechnology expanding and exposure to NPs increasing all the time, knowledge of their impact on AARSs may be used to understand the biological compatibility of NPs. Although several enzyme-NP interactions have been recently reported [15], interactions between NPs and AARSs have not been studied.

In the present study, we have chosen to explore the impact of gold (Au) and silver (Ag) NPs on one of the members of AARSs, the prolyl-tRNA synthetases (ProRSs). ProRSs catalyze the covalent attachment of the amino acid proline onto its cognate tRNA molecule in a two-step reaction [16]. The first step of the reaction is the activation of proline with ATP to give prolyl-AMP (adenylation, Equation 1), while the second step is the attachment of the prolyl group to a $tRNA^{Pro}$ molecule (aminoacylation, Equation 2). Overall, this reaction is summarized by proline, $tRNA^{Pro}$, and ATP reacting to give prolyl-$tRNA^{Pro}$, AMP and pyrophosphate (Equation 3).

$$\text{ProRS} + \text{Proline} + \text{ATP} \rightleftharpoons \text{ProRS•Prolyl-AMP} + PP_i \quad (1)$$

$$\text{ProRS•Prolyl-AMP} + tRNA^{Pro} \rightarrow \text{Prolyl-}tRNA^{Pro} + \text{AMP} + \text{ProRS} \quad (2)$$

$$\text{Net Reaction: Proline} + tRNA^{Pro} + \text{ATP} \rightarrow \text{Prolyl-}tRNA^{Pro} + \text{AMP} + PP_i \quad (3)$$

Conformational changes in protein are often associated with altered functionality. Particularly, changes in enzyme conformation may result in enhanced or diminished catalytic activity. NP-induced catalytic changes in enzymes could be used to predict potential mechanisms of NP toxicity. Alternatively, no change in catalytic function may strengthen arguments regarding nanoparticle compatibility with biological systems. The goal of this study was to determine whether AgNP and AuNP confer significant structural changes in *E. coli* ProRS and to explore the functional implications of any observed conformational changes. Intrinsic tryptophan fluorescence measurements were performed to investigate the impact NPs have on ProRS conformation. Nonradioactive and radioactive kinetic assays were performed to monitor the impact of any conformational changes on the catalytic function of ProRS. In the present study, we have monitored the first step of the aminoacylation reaction. This reaction is $tRNA^{Pro}$ independent, which considerably narrows potential complications that may arise experimentally with the abundance of negative charge within the phosphate backbone of $tRNA^{Pro}$. The second step of the aminoacylation reaction, which is $tRNA^{Pro}$ dependent, cannot take place unless the adenylation reaction occurs. Therefore, the adenylation reaction was monitored to determine catalytic implications resulting from NP exposure to *E. coli* ProRS.

2. MATERIALS AND METHODS

2.1. Nanoparticle synthesis

All chemical reagents were purchased from SIGMA-Aldrich (MO, USA), except where specifically noted. AuNP and AgNP were

synthesized as described by Sun *et al.* and Bastus *et al.*, respectively [17, 18].

2.2. Protein overexpression and purification

Plasmids encoding the ProRS construct were transformed into *E. coli* SG13009 (pREP4) (Qiagen) competent cells and grown to an A_{600} of 0.4-0.6. Protein expression was induced with 0.1 mM isopropyl β-D-thiogalactoside (IPTG) for 4 hours at 37 °C. The recombinant ProRS was purified using Co^{2+}-NTA resin (Talon) as per the manufacturer's instructions. The concentration of the purified ProRS was quantified based on active-site titration using the adenylate burst assay [19].

2.3. Intrinsic fluorescence spectroscopy

Fluorescence measurements were obtained from solutions containing Ag/Au NPs and ProRS. Each sample had a total volume of 3 mL and were prepared to contain 10 mM phosphate buffer (pH = 7.4) and 100 mM NaCl. The final concentration of ProRS used for each measurement was 5 mg/mL and the solutions contained varied NP concentrations. Concentration variation studies were performed by adding 15 nm citrate-functionalized AgNP to 3 mL samples to contain 1.5, 3.5, and 7.0 μg/mL NP; these concentrations are aligned with those reported in a recent study investigating the impact of NP on lactate dehydrogenase activity [20]. Similarly, 15 nm citrate-functionalized AuNP were added to samples to contain 11.5, 22.9, and 45.9 μg/mL NP; these concentrations were used because no change was observed between 1.5 and 7.0 μg/mL 15 nm AuNP (data not shown). Fluorescence measurements were performed using a Perkin Elmer LS55 Fluorescence Spectrometer (PerkinElmer, Inc., MA, USA) with an excitation wavelength of 280 nm at room temperature (23 °C). Emission spectra were recorded between 300 and 400 nm. All trials were performed in triplicate unless noted otherwise.

2.4. Nonradioactive enzyme kinetics

The adenylation reaction of ProRS (Equation 1) was monitored using a spectroscopic method of measuring AARSs activity outlined by Cestari *et al.* [21]. The reaction buffer consisted of 30 mM HEPES buffer (pH = 7.4), 140 mM NaCl, 30 mM KCl, and 40 mM $MgCl_2$ and included 1 mM DTT, 200 μM ATP and 2 u/mL inorganic pyrophosphatase (PPiase). Each reaction contained 40 μg/mL *E. coli* ProRS. Reactions were performed with L-proline (0.5, 1.0, 2.0, 3.0, 4.0, and 5.0 mM), 15 nm citrate-AuNP (175 μg/mL) or 15 nm citrate-AgNP (175 μg/mL). The reactions (50 μL total volume each) were performed at 37 °C in clear, flat bottom 96-well plates (Fisherbrand® 96-Well Standard Microplates) for 30 minutes. The reactions were stopped by adding 100 μL Malachite Green solution (Echelon Biosciences) and incubated for 30 minutes at room temperature. Absorbance was measured at 620 nm using a Cary 50 Microplate Reader (Varian Inc., CA, USA) after Malachite Green incubation.

2.5. Radioactive enzyme kinetics

ATP-PP_i exchange assays were performed to study the impact of NPs on the adenylation of ProRS (Equation 1). Proline concentration in the samples was 0.75 mM and WT *E. coli* ProRS concentration was 10 nM. Samples contained 50 and 200 μg/mL of Ag or Au NPs. Reactions were incubated at 37 °C for 6, 12, and 20 minutes before being quenched with 0.4 M PP_i, 15% $HClO_4$, and 3% activated charcoal [22].

3. RESULTS AND DISCUSSION

Intrinsic fluorescence spectroscopy is a technique by which the emission from aromatic amino acid side chains—phenylalanine, tyrosine, and tryptophan—is used to delineate protein conformational changes. Of the three aromatic amino acids, emission of tryptophan residues is particularly useful because of its large absorptivity, quantum yield, and overall high sensitivity to the local environment [23]. Tryptophan has a considerably high molar extinction coefficient, ε, and fluoresces with greater quantum yield than the other fluorophores. Additionally, the aromatic side chain of tryptophan is an indole ring, which contains unique spectral features distinguishing it from tyrosine. Unlike tyrosine, tryptophan emission occurs from two electronic absorption transitions, ^1L_a and ^1L_b; tyrosine emits from one transition, ^1L_b [24]. This is thought to be the reason why tyrosine emission is less sensitive to the local environment than tryptophan emission.

Given that tryptophan fluorescence is highly dependent on its micro environment, properties

including absorption and fluorescence maxima, intensity, and quantum yield have been used to decipher conformational changes in protein. Hydrogen bond interactions between tryptophan and polar molecules result in a phenomenon called fluorescence quenching. Quenching has been a useful tool in gauging the location of tryptophan fluorophores within the tertiary and quaternary structure of protein [25]. When the imino nitrogen of the indole ring participates in hydrogen bond interactions, the energy emitted from the tryptophan fluorophore is lowered. This is conventionally known as a redshift in barycentric mean fluorescence wavelength and was demonstrated by Gryczynski *et al.* in 1988. Barycentric mean fluorescence wavelength (λ_{BMF}) is the wavelength at which emission intensity is maximal (Equation 4); I(λ) is the fluorescence intensity at a given wavelength, and λ is the wavelength in nanometers.

$$\lambda_{\mathrm{BMF}} = \frac{\sum_{\lambda} \lambda \times I(\lambda)}{\sum_{\lambda} I(\lambda)} \tag{4}$$

A *redshift* in the emission spectra result in a longer λ_{BMF}, or lower energy emission, and occurs when the tryptophan residues are exposed to polar solvent. On the other hand, a *blueshift* is observed in higher energy emission spectra and occurs when tryptophan residues are excluded from solvent. In summary, tryptophan fluorescence is quenched when it is exposed to solvent [26].

An important distinction between AgNP and AuNP impact on ProRS tryptophan emission is the fact that AgNPs are consistently shown to induce a significant change in the emission spectra. Specifically, a blueshift in λ_{BMF} in the presence of AgNP is observed (Figure 1). Regardless of functionalization with citrate or polyvinylpyrrolidone (PVP), AgNP causes a blueshift in λ_{BMF} (Table 1).

In contrast, λ_{BMF} does not significantly change in the presence of AuNP (Figure 2). Functionalization of the NP does not seem to impact this result (Table 1), nor does the NP size. Citrate functionalized AuNP and AgNP of the same dimension (15 nm) cause ProRS to fluoresce differently. Samples containing 7.0 μg/mL 15 nm citrate functionalized AgNP caused the λ_{BMF} to shift by -1.39 nm, while the addition of 45.6 μg/mL 15 nm citrate functionalized AuNP caused the λ_{BMF} to shift by a mere +0.20 nm. The change in λ_{BMF} for the 15 nm AgNP sample is statistically different with respect to the control, while that of the 15 nm AuNP sample is not. The influence on ProRS conformation from AgNP is more dramatic because a far lower AgNP concentration is needed to significantly change the λ_{BMF}.

Nonradioactive kinetic analysis of the aminoacylation reaction of ProRS (Equation 1) revealed AgNP may influence catalysis, while AuNP do not (Figure 3). Using the method for measuring AARS catalytic activity described by Cestari *et al.* (2013), the adenylation reaction (Equation 1) was monitored in the presence of AgNP and AuNP using Malachite Green kinetic assays. Our studies confirmed prolyl-adenylate formation increased

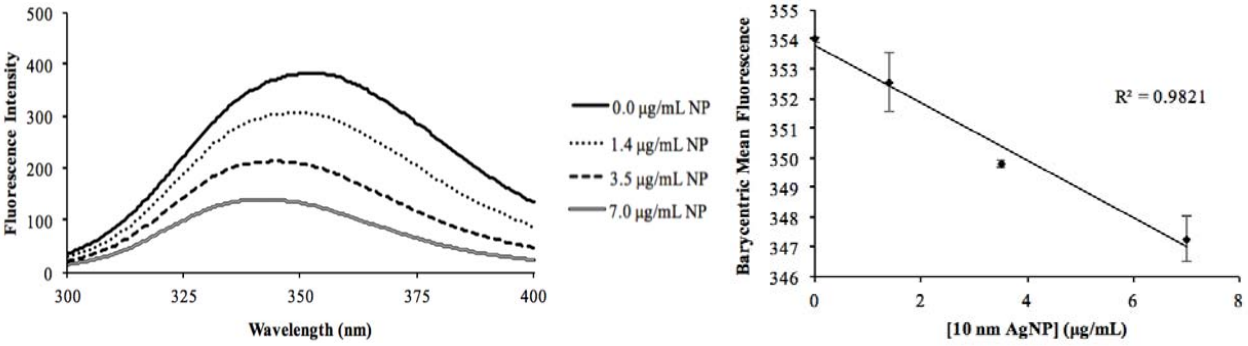

Figure 1. Fluorescence emission spectra of ProRS in the presence of 10 nm citrate-functionalized AgNP (left) and barycentric mean fluorescence wavelength (nm) of each sample as a function of concentration (right), n = 3 trials.

Table 1. Nanoparticle concentration variation fluorescence data. Nanoparticles were functionalized with citrate, mercaptoethoxy[ethoxy]ethanol (MEEE), or polyvinylpyrrolidone (PVP). $\Delta\lambda_{BMF}$ indicates the difference between λ_{BMF} of the control (0.0 μg/mL NP) and the most concentrated sample. $\Delta\lambda_{BMF}$ and R^2 is the average of three trials. *Data shown in Figure 1.

Core	Functionalization	Diameter	Concentration range	$\Delta\lambda_{BMF}$	R^2
*Silver	Citrate	10 nm	1.4-7.0 μg/mL	-6.73 nm	0.9821
Silver	Citrate	15 nm	3.0-7.0 μg/mL	-1.39 nm	0.8085
Silver	Citrate	36 nm	1.5-7.0 μg/mL	-0.66 nm	0.9997
Silver	PVP	40 nm	67.0-673.3 μg/mL	-2.44 nm	0.9830
Gold	Citrate	15 nm	11.5-45.9 μg/mL	+0.20 nm	0.8915
Gold	MEEE	15 nm	10.4-41.6 μg/mL	+0.02 nm	0.0777
Gold	MEEE	5 nm	266.0-1,067.0 μg/mL	+1.29 nm	0.7530

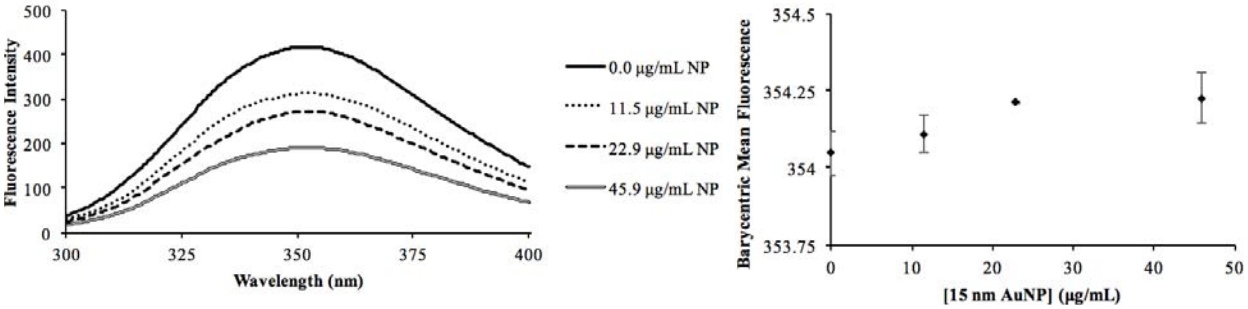

Figure 2. Fluorescence emission spectra of ProRS in the presence of 15 nm citrate-functionalized AuNP (left) and λ_{BMF} of each sample as a function of concentration (right), n = 3 trials.

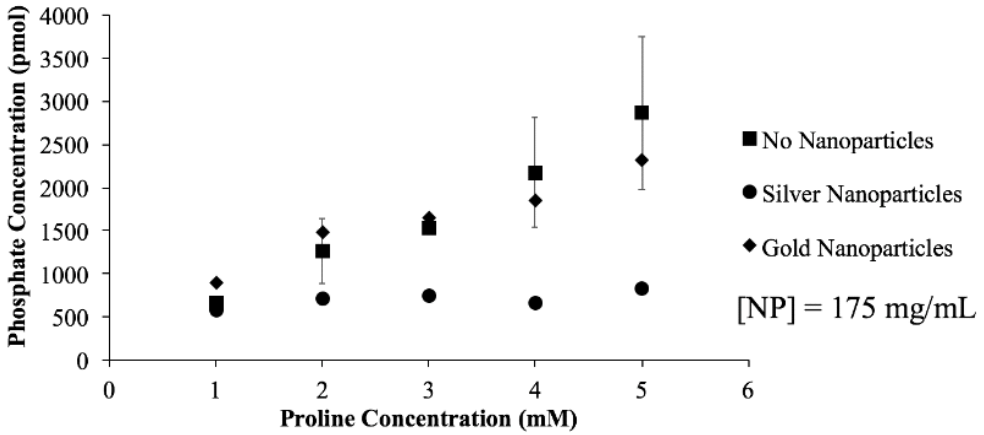

Figure 3. Nonradioactive kinetic analysis of ProRS function in nanoparticle solutions, n = 3 trials. Both AuNP and AgNP used were 15 nm and functionalized with citrate.

linearly with respect to time in the presence of each nanoparticle (data not shown). Next, substrate variation studies were performed to monitor adenylation catalysis in the presence of NP (Figure 3). These results suggested AuNPs did not significantly change the ProRS adenylation reaction; on the other hand, AgNP appeared to significantly impede ProRS adenylation activity.

As previously mentioned, the unique physio-chemical properties of NPs have prompted a variety of recent explorations in nanoscience. An interesting evolvement in the applications of NPs is the use of AgNP to absorb toxic organic dyes in water treatment facilities. Malachite Green (MG) is used commercially as a dye in commodities including leather and paper, and it is toxic to the environment. Notably, MG has been shown to adsorb onto the surface of AgNP; AgNP are now considered to be effective in removing the dye from wastewater [27]. This indicates a problem in using the MG assay in monitoring ProRS adenylation reactions and may explain why ProRS activity appears, per the nonradioactive kinetic assay results (Figure 3), to diminish in the presence of AgNP. Since AgNP and MG are known to interact with one another, a more reliable means of monitoring the enzyme kinetics must be used.

Radioactive ATP-PP_i exchange assays were performed to monitor the prolyl-adenylate formation. The assays suggest neither AuNP nor AgNP influence the adenylation reaction rate. Low concentrations (1-10 mg/mL) of AuNP and AgNP were not shown to significantly change the rate of this activation step (Figure 4). Additionally, very high and biologically irrelevant concentrations do not impact the rate either (data not shown). This is consistent with results of the nonradioactive assay study of ProRS activity in the presence of AuNP, but not with the result of ProRS activity in the presence of AgNP. Since MG has been demonstrated to adsorb onto AgNP, the results from the nonradioactive assays with AgNP cannot be acceptable. The results of the radioactive kinetic assay confirm that the Malachite Green assay is not compatible with AgNP and should be avoided in future studies of AARS catalytic function in AgNP solutions.

Although conformational changes were noticed through intrinsic fluorescence measurements in the presence of AgNPs, the absence of any significant reduction in ProRS function suggested that there is no significant alteration in the conformation of the active site pocket. Fluorescence spectra are a summation of emission from all fluorophores within the protein. For a protein with

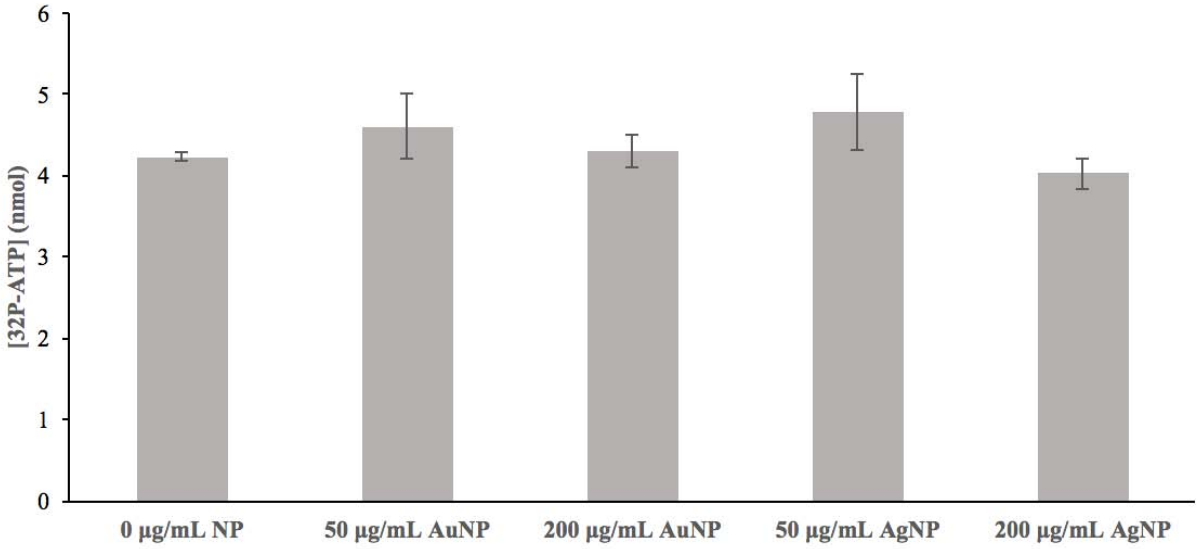

Figure 4. Radioactive kinetic analysis of ProRS adenylation reaction in 15 nm citrate functionalized AuNP and AgNP solutions (incubation time 30 minutes), n = 3 trials.

multiple tryptophan residues, it cannot be determined whether all tryptophan residues are becoming less or more exposed to solvent by the fluorescence spectra alone because the fluorescence of individual residues is impossible to monitor. Therefore, it is conceivable that some residues become more exposed to the protein surface while others become excluded from it. A net increase in emission energy (blueshift) is noticed in *E. coli* ProRS, which exists as a dimer in its natural state and each monomer consists of five tryptophan residues. The editing domain of ProRS contains one tryptophan fluorophore (TRP 375), while the rest are located within the catalytic and anticodon binding domain (Figure 5).

The tryptophan residue in the editing domain is relatively more exposed to the solvent compared to others. This residue may be responsible for the higher energy emission (blueshift) observed in the presence of AgNP if it becomes significantly more excluded from the protein surface than the other tryptophan residues. Since it is not in the catalytic domain, the changes noticed in fluorescence measurements may or may not result in observable catalytic changes for the adenylate reaction. However, it may result in other functional changes. Recently, a lysine residue in the editing domain of ProRS has been shown to be involved in editing functions of ProRS [28]. When a $tRNA^{Pro}$ molecule is acylated with any amino acid other than proline, the editing domain of *E. coli* ProRS acts to hydrolyze misacylated-$tRNA^{Pro}$. If the blueshift in λ_{BMF} in the presence of AgNP is due to conformational changes within the editing domain, editing functionality may be altered without significantly altering the prolyl-adenylate formation.

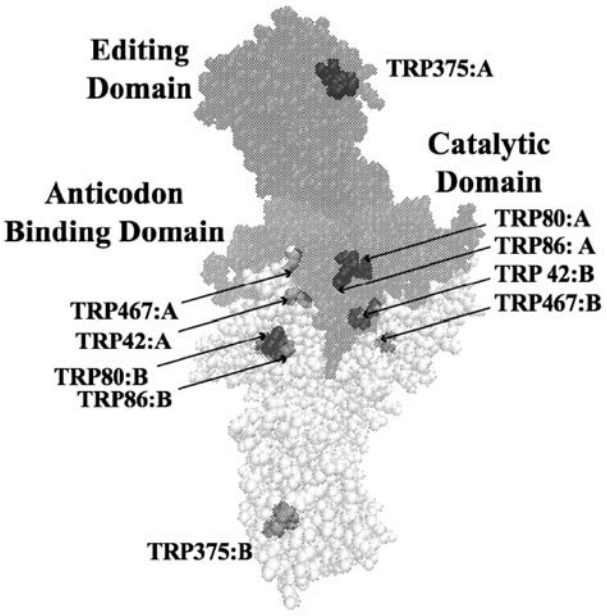

Figure 5. Visual molecular dynamics (VMD) representation of dimeric ProRS; the protein backbone of chain A (VMD Color ID 16 black/transparent) and chain B (VMD Color ID 8 white/transparent) are shown in space filled van der Waals (VDW) spheres. Tryptophan residues (VMD Color ID 16 black) are shown in space filled VDW spheres. Each of the tryptophan residues are labeled with their respective chain denoted (A or B). The three major ProRS domains are labeled on ProRS chain A.

4. CONCLUSION

In summary, AgNPs have been shown to influence the conformation of *E. coli* ProRS, while AuNP have been shown to confer no conformational change. There may be an inverse relationship between AgNP size and the degree to which the λ_{BMF} is altered in the presence of AgNP. Although we cannot rule out the possibility of having any impact of NPs on aminoacylation and/or editing function in the absence of $tRNA^{Pro}$, radioactive assays indicate there is no significant impact of AuNP or AgNP on the adenylation reaction catalyzed by *E. coli* ProRS (Equation 1). This observation is important because earlier studies have shown that the coupled dynamics between editing and catalytic domains is crucial for adenylation reaction. So, even though florescence study revealed a change in conformation of *E. coli* ProRS, the impact was not significant enough to change the coupled-domain dynamics and conformation of the catalytic domain. Therefore, there was no significant change in catalytic functions. In addition to this important observation, our study demonstrated that the procedure established by Cestari [21] for monitoring the adenylation reaction catalyzed by AARSs should not be used with AgNP because AgNP adsorb MG.

Characterizing the impact of NPs on enzyme structure and function is crucial in order to

understand the impact of NPs on biological systems. Because of the diverse range of NP applications, studies are needed to investigate NP impact on major biomolecules including metabolic enzymes, nucleic acids, lipids, and biological metabolites. These studies can lead to better understanding of NP interactions and their impact on cellular functions. Ultimately, this knowledge may be useful in generating bio-compatible nanoparticles and nanomaterials.

FUNDING

This work was supported in part by National Institute of Health [Grant Number: #1R15GM117510-0] and by the Office of Research and Sponsored Programs of the University of Wisconsin – Eau Claire, Eau Claire, WI.

CONFLICT OF INTEREST STATEMENT

The authors declare no conflict of interest.

REFERENCES

1. Sajid, M., Ilyas, M., Basheer, C., Tariq, M., Daud, M., Baig, N. and Shehzad, F. 2015, ESPR, 22(6), 4122.
2. Stark, W. J. 2011, Angew. Chem. Int. Ed., 50(6), 1521.
3. Mahmoudi, M., Lynch, I., Ejtehadi, M. R., Monopoli, M. P., Bombelli, F. B. and Laurent, S. 2011, Chem. Rev., 111(9), 5610.
4. Zeng, S., Yong, K.-T., Roy, I., Dinh, X.-Q., Yu, X. and Luan, F. 2011, Plasmonics, 6(3), 491.
5. Cho, K., Wang, X., Nie, S., Chen, Z. and Shin, D. M. 2008, Clin. Cancer Res., 14(5), 1310.
6. Fang, R. H., Jiang, Y., Fang, J. C. and Zhang, L. 2017, Biomaterials, 128, 69.
7. Nune, S. K., Gunda, P., Thallapally, P. K., Lin, Y.-Y., Forrest, M. L. and Berkland, C. J. 2009, Expert Opin. Drug Deliv., 6(11), 1175.
8. Ahamed, M. A., Mohamad, S. and Siddiqui, M. K. J. 2010, Clin. Chim. Acta, 411, 1841.
9. Maurer-Jones, M. A., Gunsolus, I. L., Murphy, C. J. and Haynes, C. L. 2013, Anal. Chem., 85(6), 3036.
10. Haley, B. and Frenkel, E. 2008, Urol. Oncol., 26(1), 57.
11. Fei, L. and Perrett, S. 2009, Int. J. Mol. Sci., 10(2), 646.
12. Wu, Z., Bin, Z. and Yan, B. 2009, Int. J. Mol. Sci., 10, 4198.
13. Lynch, I. and Dawson, K. A. 2008, Nano Today, 3(2), 40.
14. Francklyn, C. 2017, Methods, 113, 1-2.
15. Keighron, J. D. and Keating, C. D. 2010, Langmuir, 26(24), 18992.
16. Sanford, B. L., Cao, B., Johnson, J. M., Zimmerman, K., Strom, A. M. and Mueller, R. M. 2012, Biochemistry, 51(10), 2146.
17. Sun, Y. X. 2002, Science, 298, 2176.
18. Bastus, N. G., Merkocit, F., Piella, J. and Puntes, V. 2014, Chem. Mater., 26, 2836.
19. Fersht, A. R., Ashford, J. S., Bruton, C. J., Jakes, R., Koch, G. L. E. and Hartley, B. S. 1975, Biochemistry, 14(1), 1.
20. AL-Rubaee, E. A. S. 2014, GJSFR, 2(4), 111.
21. Cestari, I. and Stuart, K. 2013, J. Biomol. Screen., 18(4), 490.
22. Heacock, D. F., Forsyth, C. J., Shiba, K. and Musier-Forsyth, K. 1996, Bioorg. Chem., 24, 273.
23. Ghisaidoobe, A. B. and Chung, S. J. 2014, Int. J. Mol. Sci., 15(12), 22518.
24. Lakowicz, J. R. 2006, Principles of Fluorescence Spectroscopy, Chapter 16, 529.
25. Gryczynski, I., Wiczk, W., Johnson, M. L. and Lakowicz, J. R. 1988, Biophys. Chem., 32(2), 173.
26. Akbar, S. M., Sreeramulu, K. and Sharma, H. C. 2016, J. Bioenerg. Biomebr., 48, 241.
27. Evangelin Femila, E. M., Srimathi, R. and Charumathi, D. 2014, Int. J. Pharm. Pharm. Sci., 6(8), 579.
28. Bartholow, T. G., Sanford, B. L., Cao, B., Schmit, H. L., Johnson, J. M., Meitzner, J., Bhattacharyya, S., Musier-Forsyth, K. and Hati, S. 2014, Biochemistry, 53(6), 1059.